Orbital order in FeSe: The case for vertex renormalization

Rui-Qi Xing, Laura Classen, and Andrey V. Chubukov

Phys. Rev. B **98**, 041108 — Published 24 July 2018

DOI: 10.1103/PhysRevB.98.041108

Orbital order in FeSe – the case for vertex renormalization

Rui-Qi Xing[1], Laura Classen[2] and Andrey V. Chubukov[1]
[1] *School of Physics and Astronomy, University of Minnesota, Minneapolis, MN 55455, USA*
[2] *Condensed Matter Physics and Materials Science Department, Brookhaven National Laboratory, Upton, NY 11973-5000, USA*

We study the structure of the orbital order $\Gamma = \langle d^\dagger_{xz} d_{xz} - d^\dagger_{yz} d_{yz} \rangle$ in FeSe in light of recent STM and ARPES data, which detect the shapes of hole and electron pockets in the nematic phase. The geometry of the pockets indicates that the sign of Γ is different between hole and electron pockets (Γ_h and Γ_e). We argue that this sign change cannot be reproduced if one solves for the orbital order within mean-field approximation, as the mean-field analysis yields either no orbital order, or order with the same sign of Γ_e and Γ_h. We argue that another solution with the opposite signs of Γ_e and Γ_h emerges if we include the renormalizations of the vertices in $d-$wave orbital channel. We show that the ratio $|\Gamma_e/\Gamma_h|$ is of order one, independent on the strength of the interaction. We also compute the temperature variation of the energy of d_{xz} and d_{yz} orbitals at the center of electron pockets and compare the results with ARPES data.

Introduction Orbital degrees of freedom turned out to play an important role for iron-based superconductors (FeSC). Studies of SDW magnetism and superconductivity in these materials found that the orbital composition of the states near the Fermi surface (FS) affects the structure of the fermionic spectrum in the spin-density-wave (SDW) phase [1] and the anisotropy of the superconducting gap [2–4]. Another example is the tetragonal-to-orthorhombic phase transition observed in many FeSCs at $T = T_s$. Below T_s, the system spontaneously breaks C_4 lattice rotational symmetry down to C_2. Below T_s the occupation of d_{xz} and d_{yz} orbitals becomes unequal, i.e., the system develops an orbital order $\Gamma(|\mathbf{k}|) \propto \int d\theta_k (n_{xz}(\mathbf{k}) - n_{yz}(\mathbf{k}))$, where n_i is the density of orbital i, and the integration is over the directions of $\mathbf{k}$ for a given $|\mathbf{k}|$. Above T_s, Γ_k vanishes by C_4 symmetry, but once C_4 symmetry is broken, by one reason or the other [5], $\Gamma(|\mathbf{k}|)$ becomes finite.

In most FeSCs the range of nematic order is quite narrow as the system develops a stripe magnetic order almost immediately after the nematic order sets in. However, in FeSe (and in doped $FeSe_{1-x}S_x$) the regions of nematic and magnetic order are well separated ([6, 7]). In pure FeSe, the nematic order sets in at $T_s \approx 85K$, and magnetic order does not develop down to $T = 0$. This opens up an opportunity to extract the information about the structure of Γ from the analysis of the feedback effects on the electronic structure. The magnitude of Γ, extracted from ARPES, is $10 - 20meV$, much smaller than the fermionic bandwidth [6, 8–15]. In this case, the most relevant feedback from Γ is on fermions near hole and electron pockets. The pockets in FeSe are quite small, and $\Gamma(|\mathbf{k}|)$ near these pockets is well approximated by numbers Γ_h and Γ_e.

Manifestations of the orbital order in FeSe have been seen in Raman, STM, ARPES, and other experiments (see Ref. [6] for recent review on FeSe). STM and ARPES data show [8–12, 16] that below T_s the larger hole pocket becomes elliptical and $(\pi, 0)$ electron pocket becomes peanut-like. Adding Γ_h and Γ_e terms to the hopping Hamiltonian in orbital representation and transforming from orbital to band basis, one can make sure [8, 17] that the observed shapes of the pockets are reproduced if $\Gamma_h > 0$ and $\Gamma_e < 0$, i.e., the orbital order changes sign between hole and electron pockets.

In this communication we consider how the sign change between Γ_e and Γ_h can be understood theoretically. For this, we derive and analyze the self-consistent equation for d-wave orbital order Γ. We argue that at mean-field level, the set of coupled equations for Γ_h and Γ_e contains the single effective interaction $U_0 = 5J - U$, where U and J are Hubbard and Hund local interactions. The orbital order either does not develop, when $U_0 > 0$, or yields equal sign of Γ_e and Γ_h, when $U_0 < 0$. We next include into the analysis the fact that the couplings flow away from their bare values (used in mean-field analysis), when we progressively integrate out contributions of fermions with higher energies. This flow is captured within parquet renormalization group analysis (pRG) [18] or functional RG [19]. The pRG flow splits U_0 into two different interactions U_a and U_b. We show that this splitting gives rise to a non-zero coupling in another channel for orbital ordering, this time with Γ_e and Γ_h of opposite signs (d^{+-} channel). This is similar to how the coupling in the s^{+-} pairing channel emerges due to small inter-pocket pairing interaction on top of strong Hubbard repulsion. We show that the coupling in this new orbital channel is attractive, regardless of the sign of the bare U_0, and exceeds the coupling in the d^{++} channel. Our results are summarized in Figs. 2, 3.

Our approach is similar to earlier works [4, 20], which also found an attraction in the d^{+-} channel, but differs in detail. The authors of [4] analyzed the flow of the interactions in the C_4 symmetric regime near the fixed trajectory, i.e., at the very end of the pRG flow. Here we consider the evolution of U_a and U_b without assuming a special relation between the interactions in the universal regime close to a fixed trajectory. This is a more realistic approach, given that in practice pRG only runs over a finite window of energies. We show that the d^{+-} channel becomes attractive from the very beginning of the pRG flow. In another distinction with [4] here we consider the

ordered phase and include the splitting between d_{xz} and d_{yz} orbitals and nematicity-induced changes to Bogoliubov coefficients of the transformation from the orbital to the band basis. The authors of [20] considered the case of large $U/J > 5$ and obtained sign-changing d^{+-} orbital order by selecting a particular combination of RPA and Aslamazov-Larkin type diagrams for the renormalization of the Hubbard interaction. We consider arbitrary U/J and treat vertex renormalizations within pRG, which accounts on equal footing for vertex renormalizations in particle-hole and particle-particle channels. We find that it is important to include the full renormalization because the sign change between Γ_h and Γ_e depends on the level of approximation. Another explanation for the sign change between Γ_e and Γ_h has been put forward in Ref. [21]. It is based on the earlier study[22], which showed that the self-energy due to spin fluctuation exchange has opposite sign near Γ and near X/Y, and shrinks both hole and electron pockets. Our approach is complimentary to that work: we include orbital order into fermionic propagators, but neglect nematicity-induced changes of the interactions, while the authors of [21] included the X/Y anisotropy of the effective interaction but not orbital order. We emphasize that both approaches lead to sign-changing orbital order.

We also consider how orbital order affects the energies of d_{xz} and d_{yz} orbitals E_{xz} and E_{yz} at $(0,\pi)$ and $(\pi,0)$ points in the 1FeBZ. In absence of orbital order, the two energies are degenerate even in the presence of spin-orbit coupling[23]. A non-zero Γ_e breaks the degeneracy. To first order in Γ_e, E_{xz} increases by $\Gamma_e/2$ and E_{yz} decreases by $\Gamma_e/2$. Observation of this splitting has been reported in Refs. [13, 16], but not in Ref.[10]. The authors of [13, 16] argued that the d_{xz}/d_{yz} splitting appears on top of a larger effect – a simultaneous change of the temperature dependence of E_{xz} and E_{yz} below T_s. To verify this claim, we compute the corrections to E_{xz} and E_{yz} to second order in Γ_e and Γ_h. The Γ_e^2 and Γ_h^2 terms are the same for E_{xz} and E_{yz} and, if these terms are large, they can overtake the $\pm\Gamma_e/2$ splitting already at small Γ_i. We find that the second order contribution accounts only for a small correction to $\pm\Gamma_e/2$. If both E_{xz} and E_{yz} indeed become smaller in magnitude below T_s, as the authors of [13, 16] argue, this must be due to some other physics.

ψ_i	Pocket	Orbital	ψ_i	Pocket	Orbital	ψ_i	Pocket	Orbital
ψ_1	Y	d_{xz}	ψ_3	X	d_{yz}	ψ_5	Γ	d_{yz}
ψ_2	Y	d_{xy}	ψ_4	X	d_{xy}	ψ_6	Γ	d_{xz}

TABLE I. Affiliation of ψ_i with a pocket and an orbital.

Mean-field analysis We consider a model with two hole pocket near $(0,0)$ in the tetragonal phase (H-pockets) and two electron pockets near $(0,\pi)$ and $(\pi,0)$ in the 1FeBZ (Y and X pockets). The hole pockets are made out of d_{xz} and d_{yz} orbitals, the X pocket is made out of d_{yz} and d_{xy} orbitals and the Y pocket is made out of d_{xz} and d_{yz} (Refs. [2, 24]). We introduce six spices of fermions: $\psi_1,\dots,\psi_6$, see Tab I and two $d-$wave d_{xz}/d_{yz} orbital order parameters $\Gamma_h = \langle\psi_6^\dagger\psi_6 - \psi_5^\dagger\psi_5\rangle$ and $\Gamma_e = \langle\psi_1^\dagger\psi_1 - \psi_3^\dagger\psi_3\rangle$. For simplicity, we neglect d-wave orbital order on the d_{xy} orbital (the $\psi_2^\dagger\psi_2 - \psi_4^\dagger\psi_4$ term, Refs. [23, 25]). At the mean-field level, the self-consistent equations for Γ_h and Γ_e are obtained by adding up Hartree and Fock diagrams for different orbitals (Fig. 1a). To first order in the orbital order parameter, the self-energies are $\Sigma_{xz}^H = \Sigma_{h,0} + \Gamma_h/2$, $\Sigma_{yz}^H = \Sigma_{h,0} - \Gamma_h/2$, $\Sigma_{xz}^Y = \Sigma_{e,0} + \Gamma_e/2$, $\Sigma_{yz}^X = \Sigma_{e,0} - \Gamma_e/2$, where $\Sigma_{h,0}$ and $\Sigma_{e,0}$ are the self-energies in the absence of orbital order. Evaluating the diagrams and taking the difference $\Sigma_{xz}^H - \Sigma_{yz}^H = \Gamma_h$, $\Sigma_{xz}^Y - \Sigma_{yz}^X = \Gamma_e$, we obtain self-consistent equations for Γ_h, Γ_e in the form [26]

$$\begin{aligned}\Gamma_h &= U_a\left(n_{xz}^H - n_{yz}^H\right) + U_b\left(n_{xz}^Y - n_{yz}^X\right)\\ \Gamma_e &= U_a\left(n_{xz}^Y - n_{yz}^X\right) + U_b\left(n_{xz}^H - n_{yz}^H\right)\end{aligned} \tag{1}$$

Here each density n_i is the momentum integral over the corresponding Fermi function. We find, to leading order in Γ_i, $n_{xz}^H - n_{yz}^H = A_h\Gamma_h$ and $n_{xz}^Y - n_{yz}^X = A_e\Gamma_e$. To obtain the prefactors A_h and A_e, we used the orbitally-resolved low-energy model from Ref. [24] for the kinetic energy, converted from orbital to band basis, and computed the momentum integrals of the Fermi functions for different bands. Finite values of Γ_h and Γ_e split the energies of d_{xz} and d_{yz} orbitals and affect the Bogoliubov coefficients of the orbital-to-band transformation. They also modify the interactions U_a and U_b, but to linear order in Γ_e and Γ_h, U_a and U_b in (1) can be evaluated in the tetragonal phase.

We present the details of the calculations in [27] and here state the result: both A_h and A_e are negative, and their ratio $\gamma = A_e/A_h$ depends on the parameters in the kinetic energy and is, in general, of order one. Using the band structure parameters that fit the ARPES and STM data, we obtained $\gamma \sim 0.2$.

The interactions U_a and U_b are linear combinations of seven interactions involving d_{xz} and d_{yz} orbital states near momenta where FSs are located. We show these seven interactions in Fig. 1b. In terms of these interactions, $U_a = U_5 - 2\tilde{U}_5 + \tilde{\tilde{U}}_5$[28] and $U_b = 2(U_1 - \bar{U}_1) - (U_2 - \bar{U}_2)$ (labels are as in Fig. 1b). The bare values of the interactions are $U_5^{(0)} = U_1^{(0)} = U_2^{(0)} = U, \tilde{U}_5^{(0)} = \bar{U}_1^{(0)} = U', \tilde{\tilde{U}}_5^{(0)} = \bar{U}_2^{(0)} = J$. As a result, the bare $U_a^{(0)}$ and $U_b^{(0)}$ are the same: $U_a^{(0)} = U_b^{(0)} = U_0 = U + J - 2U'$. If we take $U' = U - 2J$ (Ref. [2]), we obtain $U_0 = 5J - U$. Substituting $U_a = U_b = U_0$ into (1), we obtain that the only possible solution of the self-consistent set is $\Gamma_h = \Gamma_e$ (sign-preserving d^{++} orbital order), and this order develops if the eigenvalue $\lambda^{++} = U_0(A_h + A_e) > 1$. The solution with the opposite sign of Γ_e and Γ_h does not emerge at the mean-field level.

Beyond mean-field We now go beyond mean-field and include into consideration that the seven in-

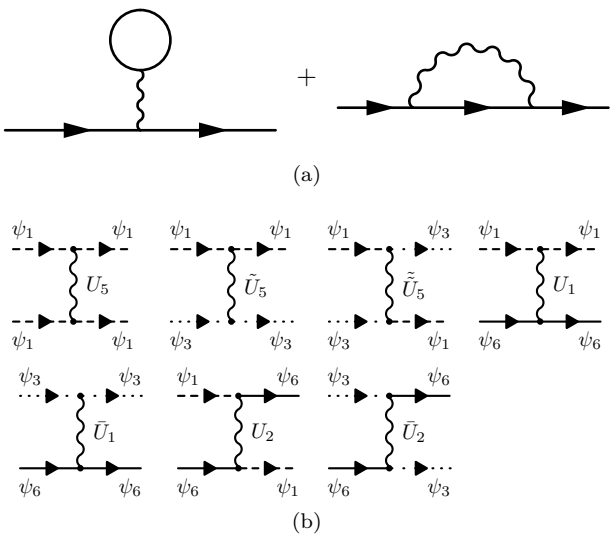

FIG. 1. a) Hartree and Fock self-energy diagrams; b) Examples of the interaction terms which contribute to Hartree-Fock self-energies. The U_5 terms in the first row also act on hole pockets (ψ_5, ψ_6). Each diagram has symmetry-equivalents. $(\psi_1 \leftrightarrow \psi_3,\ \psi_5 \leftrightarrow \psi_6)$. The self-energy beyond mean-field has been computed using dressed interactions, which we obtained using pRG scheme. In a direct perturbation theory, this amounts to summing up infinite series of self-energy diagrams, including RPA and Aslamazov-Larkin diagrams.

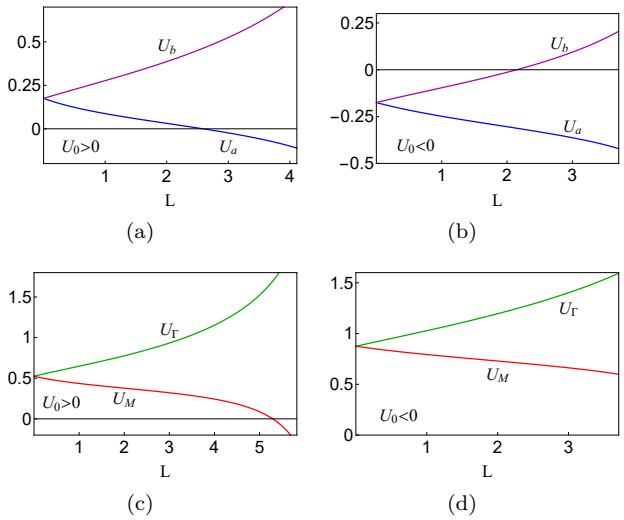

FIG. 2. Panels (a) and (b) – the pRG flow of the couplings U_a and U_b for the case when the bare $U_a^{(0)} = U_b^{(0)} = U_0 = 5J - U$ is positive in (a) and negative in (b) (we set $J/U = 0.3$ and 0.1, respectively). Panels (c) and (d) – the flow of the couplings U_M and U_Γ in Eq. (3). The parameter $L = log\frac{W}{E}$, where W is of order bandwidth and E is the running energy. The larger L is, the more high energy states are integrated out. We used $m_h U/(4\pi) = 0.35$ where m_h is the mass of the dispersion near the hole pocket.

teractions, which contribute to U_a and U_b, flow to different values as one progressively integrates out fermions with higher energies. This flow can be captured within pRG and comes from mutual vertex renormalizations of the total of 30 different interactions between low-energy fermions on d_{xz}, d_{yz}, and d_{xy} orbitals [4, 24, 25]. The flow equations have been derived in [25], and we use the results of that work to obtain the flow of U_a and U_b. This flow accounts for the full logarithmically singular vertex renormalizations in the particle-hole and particle-particle channels.

The results are shown in Fig.2. We see that U_a and U_b become different from U_0, and $U_b > U_a$, irrespective of whether $U_0 > 0$ or $U_0 < 0$. Solving for the eigenfunctions and eigenvalues of Eq. (1) when U_a and U_b are different, we obtain an eigenfunction $\Gamma^{++} = \Gamma_h + \alpha_+\Gamma_e$ with the eigenvalue λ^{++} and $\Gamma^{+-} = \Gamma_h + \alpha_-\Gamma_e$ with the eigenvalue λ^{+-}, where

$$\alpha_\pm = -\frac{1-\gamma}{2}\frac{U_a}{U_b} \pm \sqrt{\left(\frac{1-\gamma}{2}\right)^2 \frac{U_a^2}{U_b^2} + \gamma} \qquad (2)$$

$$\lambda^{++,+-} = -|A_h| \left[\frac{1+\gamma}{2}U_a \pm U_b\sqrt{\left(\frac{1-\gamma}{2}\right)^2 \frac{U_a^2}{U_b^2} + \gamma}\right]$$

We see that $\alpha_+ > 0$ and $\alpha_- < 0$, i.e., the eigenfunction Γ^{++} describes sign-preserving d^{++} orbital order and Γ^{+-} describes sign-changing d^{+-} order. We plot the corresponding eigenvalues λ^{++} and λ^{+-} in Fig. 3. We see that λ^{+-} becomes positive (i.e., attractive) for any sign of U_0, once we include the pRG flow of the interactions. We emphasize that this holds even if the flow runs only over a small range of energies. For an instability towards a sign-changing orbital order, the flow needs to run over a finite range of energies to reach $\lambda^{+-} > 1$.

For $U_0 > 0$, the coupling in the λ^{++} channel is repulsive, i.e., d^{+-} orbital order is the only solution of Eq. (1). For $U_0 < 0$, the d^{++} channel is attractive at the bare level, but we see from Fig. 3c,d that it becomes sub-leading once U_b changes sign under pRG (see Fig. 2b). The attraction in d^{+-} orbital channel for $U_0 < 0$ was earlier obtained in Ref. [20] who used a combination of RPA spin and charge channels and Aslamazov-Larkin diagrams to separate U_a and U_b. In distinction with Ref. [20], here we account for the renormalization of U_a and U_b systematically, in an order-by-order treatment (as pRG is), through all channels including the pairing channel. Like we said, we found that λ^{+-} becomes positive already at the very beginning of the pRG flow, when the renormalization of $U_{a,b}$ can be obtained within a direct perturbative expansion. In particular, the condition $U_0 < 0$ is not required [29]. We note that our computation of the self-energy, using the diagrams in Fig. 1a with the dressed interactions is diagrammatically equivalent to summing up infinite series of contributions to the self-energy, including both RPA and Aslamazov-Larkin diagrams.

Temperature variations of E_{xz} and E_{yz}. We now analyze how the energies E_{xz} at $(0, \pi)$ and E_{yz} at

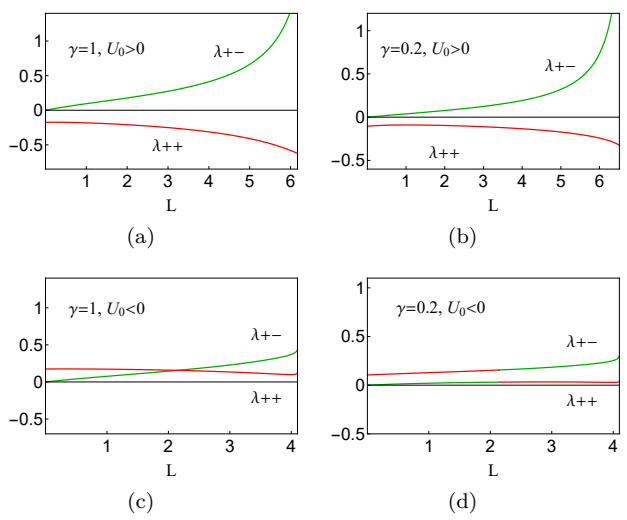

FIG. 3. The flow of the dimensionless couplings λ^{++} in sign-preserving d^{++} channel (green) and λ^{+-} in sign-changing d^{+-} channel (red). Notations are as in Fig. 2. Panels (a) and (b) - the flow for the case $U_0 = 5J - U > 0$ for two values of the parameter $\gamma = A_e/A_h$ (see text). Panels (c) and (d) – the same for $U_0 < 0$. The sign-changing d^{+-} channel becomes dominant once U_b changes sign near $L = 2$. . For $\gamma \neq 1$, the couplings jump by finite values when U_b passes through zero.

$(\pi, 0)$ vary with increasing orbital order (in the 2FBZ these are energies of d_{xz}/d_{yz} orbitals at M). To first order in Γ_e, the two energies just split: $E_{xz} = E_{e,0} + \Gamma_e/2$ and $E_{yz} = E_{e,0} - \Gamma_e/2$, where $E_{e,0} < 0$ is the energy in the absence of the nematic order [23, 24]. Our goal is to go beyond the first order in Γ_e and check if there is a large common term of order $\Gamma^2_{e,h}$. To check this, we computed the self-energies Σ^Y_{xz} and Σ^X_{yz} to order Γ^2. We We did not do the full self-consistent calculation to this order, as it would require to include the self-energy to order Γ^2 into the densities $n^H_{xz}, n^H_{yz}, n^Y_{xz}$, and n^X_{yz}. Rather, we evaluated the "source" term in the self-energy $\Sigma_{so}(\Gamma)$, which comes from keeping $O(\Gamma_{h,e})$ terms in the self-energy, but expanding the densities to order $\Gamma^2_{h,e}$. The the common self-energy for Σ^Y_{xz} and Σ^X_{yz} below the nematic transition is proportional to $\Sigma_{so}(\Gamma) - \Sigma_{so}(0)$. We find

$$\Sigma_{so}(\Gamma) = U_M(n^Y_{xz} + n^X_{yz}) + U_\Gamma(n^H_{xz} + n^H_{yz}) \qquad (3)$$

and $U_M = U_5 + 2\tilde{U}_5 - \tilde{\tilde{U}}_5$ and $U_\Gamma = 2(U_1 + \bar{U}_1) - (U_2 + \bar{U}_2)$. The bare value of U_M and U_Γ are again equal, each is $U + 2U' - J$ $(= 3U - 5J$ if $U' = U - 2J)$, but under pRG, U_Γ becomes larger than U_M, as we show in Fig. 2 c,d. The common densities are $(n^H_{xz} + n^H_{yz}) = n_{h,0} + B_h\Gamma^2_h, (n^Y_{xz} + n^X_{yz}) = n_{e,0} + B_e\Gamma^2_e$, where $n_{i,0}$ labels the density for $\Gamma_i = 0$. We find (see [27] for details) that the magnitudes of B_h and B_e are at most of order $1/T_s$, hence near T_s, when $\Gamma_{h,e}$ are small, the self-energy to second order in Γ_i is a small correction to the first-order $\pm\Gamma_i/2$ term. This is inconsistent with the interpretation of the data in Refs. [13, 16].

Conclusions. In this communication we presented the solution of self-consistent equations for d-wave nematic order parameters on d_{xz}/d_{yz} orbitals. We argued that at a mean-field level the only solution possible is sign-preserving d^{++} nematic order Γ (same sign of Γ_e and Γ_h) when the bare coupling $U_0 < 0$. We went beyond mean-field and included the flow of the couplings under pRG. Then we found an attraction in d^{+-} channel for which Γ_e and Γ_h have opposite sign, in agreement with STM and ARPES data. We argued that d^{+-} orbital order becomes the leading instability for either sign of bare U_0. We also computed the common self-energy for d_{xz} and d_{yz} orbitals at the center of electron pockets to second order in Γ to check whether we can reproduce the results of Refs. [13, 16] that the energies E^Y_{xz} and E^X_{yz} simultaneously get smaller by magnitude in the nematic phase. We obtained a much smaller self-energy and of opposite sign than the one which is needed. If the interpretation of the data in[13, 16] is correct, it has to be due to a self-energy with vertices beyond our RG analysis.

ACKNOWLEDGMENTS

We thank A. Coldea, L. Basconses, L. Benfatto, S. Borisenko, D. Chichinadze, R.M. Fernandes, J. Kang, T.K. Kim, W. Ku, L. de' Medici, M. Watson, and Y.M. Wu for useful discussions. R.X. and A.V.C. are supported by the Office of Basic Energy Sciences, U.S. Department of Energy, under award DE-SC0014402. L.C. acknowledges support from the Alexander-von-Humboldt foundation. Work at BNL is supported by the U.S. Department of Energy (DOE), Division of Condensed Matter Physics and Materials Science, under Contract No. DE-SC0012704. Part of the work was done while A.V.C. was visiting KITP in Santa Barbara. KITP is supported by NSF under Grant No. NSF PHY17-48958. RX and LC equally contributed to this project.

[1] Ying Ran, Fa Wang, Hui Zhai, Ashvin Vishwanath, Dung-Hai Lee, Phys. Rev. B 79, 014505 (2009).
[2] S. Graser, T. A. Maier, P. J. Hirschfeld, and D. J. Scalapino, New J. Phys. 11, 025016 (2009).
[3] Naoya Arakawa, Masao Ogata, J. Phys. Soc. Jpn. 80, 074704 (2011)
[4] A. V. Chubukov, M. Khodas, R. M. Fernandes, Phys. Rev. X **6**, 041045 (2016).
[5] R. M. Fernandes and A. V. Chubukov, Rep. Prog. Phys. **80**, 014503 (2017).
[6] see e.g., Anna E. Böhmer, Andreas Kreisel, Journal of Physics: Condensed Matter 30, 023001 (2017) and refer-

ences therein.
[7] K. Matsuura, Y. Mizukami, Y. Arai, Y. Sugimura, N. Maejima, A. Machida, T. Watanuki, T. Fukuda, T. Yajima, Z. Hiroi, K. Y. Yip, Y. C. Chan, Q. Niu, S. Hosoi, K. Ishida, K. Mukasa, S. Kasahara, J.-G. Cheng, S. K. Goh, Y. Matsuda, Y. Uwatoko, and T. Shibauchi, Nature Communications, 8 1143 (2017).
[8] P. O. Sprau, A. Kostin, A. Kreisel, A. E. BÃ¶hmer, V. Taufour, P. C. Canfield, S. Mukherjee, P. J. Hirschfeld, B. M. Andersen, and J. C. Seamus Davis, Science **357**, 6346 (2017).
[9] H. C. Xu, X. . Niu, D. F. Xu, J. Jiang, Q. Yao, Q. Y. Chen, Q. Song, M. Abdel-Hafiez, D. A. Chareev, A. N. Vasiliev, Q. S. Wang, H. L. Wo, J. Zhao, R. Peng, and D. L. Feng, Phys. Rev. Lett. **117**, 157003 (2016) T. Hashimoto, Y. Ota, H. Q. Yamamoto, Y. Suzuki, T. Shimojima, S. Watanabe, C. Chen, S. Kasahara, Y. Matsuda, T. Shibauchi, K. Okazaki, and S. Shin, Nat. Comm. **9**, 282 (2018);
[10] M. D Watson, A. A. Haghighirad, L. C. Rhodes, M. Hoesch, T. K. Kim, New J. Phys. **19**, 103021 (2017)
[11] Y. Suzuki, T. Shimojima, T. Sonobe, A. Nakamura, M. Sakano, H. Tsuji, J. Omachi, K. Yoshioka, M. Kuwata-Gonokami, T. Watashige, R. Kobayashi, S. Kasahara, T. Shibauchi, Y. Matsuda, Y. Yamakawa, H. Kontani, and K. Ishizaka, Phys. Rev. B **92**, 205117 (2015).
[12] Xingjiang Zhou, private communication
[13] A. Fedorov, et al., Scientific Reports **6**, 36834(2016).
[14] A. Coldea and M. Watson, Annual Review of Condensed Matter Physics 9, 125 (2018).
[15] In some earlier studies, see e.g., Ref. [21] a larger magnitude of $\Gamma_e \sim 50meV$ has been reported. The authors of later studies argued [10, 13, 14] that $50meV$ is the difference between the energies of d_{xz}/d_{yz} and d_{xy} orbitals.
[16] Y. S. Kushnirenko, A. V. Fedorov, E. Haubold, S. Thirupathaiah, T. Wolf, S. Aswartham, I. Morozov, T. K. Kim, B. Buchner, and S. V. Borisenko, arXiv:1802.08668.
[17] J. Kang, R.M. Fernandes, and A.V. Chubukov, arXiv:1802.01048.
[18] A.V. Chubukov, Annul. Rev. Cond. Mat. Phys.3, 13.1 (2012).
[19] Fa Wang, Hui Zhai, Ying Ran, Ashvin Vishwanath, Dung-Hai Lee, Physical Review Letters, 102, 047005 (2009); Christian Platt, Werner Hanke, Ronny Thomale, Advances in Physics 62, 453-562 (2013).
[20] S. Onari, Y. Yamakawa, and H. Kontani, Phys. Rev. Lett. **116**, 227001 (2016).
[21] L. Fanfarillo, J. Mansart, P. Toulemonde, H. Cercellier, P. Le Fevre, F. Bertran, B. Valenzuela, L. Benfatto, V. Brouet, Phys. Rev. B **94**, 155138 (2016)
[22] L. Ortenzi, E. Cappelluti, L. Benfatto and L. Pietronero, Phys. Rev. Lett. **103**, 046404 (2009).
[23] R. M. Fernandes and O. Vafek, Phys. Rev. B **90**, 214514(2014)
[24] V. Cvetkovic and O. Vafek, Phys. Rev. B **88**, 134510 (2013).
[25] R.-Q. Xing, L. Classen, M. Khodas, A. V. Chubukov, Phys. Rev. B **95**, 085108 (2017); L. Classen, R.-Q. Xing, M. Khodas, A. V. Chubukov, Phys. Rev. Lett. 118, 037001 (2017).
[26] In principle, the r.h.s. of Eq. (1) also contains the term $n^Y_{xy} - n^X_{xy}$ as this difference has a piece linear in Γ_e. However this term turns out to be numerically smaller than $n^Y_{xz} - n^X_{yz}$ already at a bare level and we neglect it. Another reason to neglect the contribution from d_{xy} orbital is that for $U > U'$, interactions involving fermions from d_{xy} orbital flow under pRG to progressively smaller values than the ones involving fermions from d_{xz}/d_{yz} orbital. The smallness of the interactions involving d_{xy} orbital also follows from other treatments [Z. P. Yin, K. Haule, G. Kotliar, Nature Materials **10**, 932 (2011); L. de' Medici, G. Giovannetti, M. Capone, Phys. Rev. Lett. **112**, 177001 (2014); E. Bascones, B. Valenzuela, and M. J. Calderon, Phys. Rev. B **86**, 174508 (2012); L. Fanfarillo, G. Giovannetti, M. Capone, E. Bascones, Phys. Rev. B **95**, 144511 (2017)].
[27] See Supplementary Material
[28] In principle, one has to distinguish between interactions on hole and electron pockets for U_a. However, they differ only by a factor [25]. To smplify the presentation, in the main text we set U_a to be equal on hole and electron pockets. We discuss a generic case in [27].
[29] The authors of [20] found that the attraction in d^{+-} channel holds also for $U_0 > 0$ (H. Kontani, private communication).